Orientational Order of Difluorinated Liquid Crystals: A Comparative 13 C-NMR, Optical, and Dielectric Study in Nematic and Smectic B Phases

ARTICLE *in* THE JOURNAL OF PHYSICAL CHEMISTRY B · AUGUST 2008

Impact Factor: 3.3 · DOI: 10.1021/jp800378g · Source: PubMed

Orientational Order of Difluorinated Liquid Crystals: A Comparative ^{13}C-NMR, Optical, and Dielectric Study in Nematic and Smectic B Phases

M. Geppi,*,† A. Marini,†,‡ C. A. Veracini,† S. Urban,§ J. Czub,§ W. Kuczyński,|| and R. Dabrowski⊥

Dipartimento di Chimica e Chimica Industriale, Università di Pisa, Via Risorgimento 35, 56126 Pisa, Italy, Scuola Normale Superiore, Piazza dei Cavalieri 15, 56126, Pisa, Italy, Institute of Physics, Jagiellonian University, Reymonta 4, 30-059, Kraków, Poland, Institute of Molecular Physics, Polish Academy of Sciences, Smoluchowskiego 17, 60179, Poznań, Poland, and Institute of Chemistry, Military University of Technology, 00-908 Warszaw, Poland

Received: January 15, 2008; Revised Manuscript Received: May 5, 2008

Structural and orientational order properties of **3Cy2CyBF2** and of **5CyCy2BF2** have been investigated by means of ^{13}C-NMR, optical, and dielectric spectroscopy methods. In the case of NMR, order parameters have been independently obtained from the analysis of either ^{13}C-^{19}F dipolar couplings or ^{13}C chemical shift anisotropies, both measured from ^{13}C-{^{1}H} NMR static spectra. The assignment of the ^{13}C resonances has been carried out thanks to the comparison with solution state spectra and DFT calculations, and the relevant geometrical parameters and ^{13}C chemical shift tensors needed to derive orientational order parameters have been calculated by DFT methods. In the analysis of ^{13}C-^{19}F dipolar couplings, empirical corrections for vibrations and anisotropic scalar couplings have been included. Dielectric measurements have been performed over a broad frequency range for two orientations of the nematic director with respect to the measuring field. At low frequencies (static case) a positive dielectric anisotropy has been determined, which has enabled the calculation of the order parameters according to a well-tested procedure. At high frequencies the dielectric anisotropy changes its sign, a property which can be useful in designing a dual addressing display. The nematic order parameter determined from optical, dielectric, and NMR methods have been compared: their trends with temperature are very similar, apart from some slight shifts, and were analyzed by Haller and Chirtoc models. The differences among the results obtained by the four methods have been discussed in detail, also with reference to the assumptions and approximations used in each case, and to the results recently reported for similar fluorinated nematogens. The presence of a non-negligible order biaxiality has been related to the presence of a CH_2CH_2 bridging group, linking one cyclohexylic unit with either the other cyclohexyl or the phenyl ring.

1. Introduction

The introduction of fluorine atoms in liquid crystalline materials gives them particular properties as compared to their hydrocarbon homologues. In the last two decades the use of organofluorine compounds has generated a strong research effort, not only for liquid crystal displays (LCDs) but also for other technological applications. It has been demonstrated that the replacement of one or a few hydrogen atoms with fluorine ones may confer to the resulting material unusual and peculiar properties, which allow its use as surface coating, fire retardants, and in biomedicine.[1] In the field of liquid crystals (LCs), fluorinated materials are mainly used in display devices such as twisted nematic liquid crystals display (TNLCD), active matrix liquid crystals display (AM-LCD), or for the development of surface stabilized ferroelectric smectic C* display (SSFLCDs). Much attention is paid to fluorinated nematogens, because they often have broad nematic mesophase ranges, low rotational viscosity, low conductivity, and high dielectric anisotropy.[2] Furthermore, the controlled choice of the molecular position of fluorine atoms allows tailoring of appropriate dielectric anisotropies for commercial applications.[3] However, the impact of fluorine in this field has been, up to now, little studied in comparison to other effects observed in LCs. In a recent paper, we have shown how the use of different spectroscopic techniques can provide insights at a molecular level on these fluorinated materials.[4] Following the trail of our previous work, structural and orientational order properties of two difluorinated nematogens (one of which also shows a smectic B phase) have been studied by means of optical, dielectric, and ^{13}C-NMR techniques. With respect to the mesogens investigated in ref 4, the two molecules here investigated differ for the presence of a CH_2CH_2 bridging group, in one case situated between the difluorinated phenyl ring and a cyclohexyl group, in the other case between two cyclohexyl groups, one of which directly linked to the phenyl ring. Moreover, in the present work, in addition to what done in ref 4, order parameters were also derived using ^{13}C chemical shift anisotropies. Given the similar approaches followed here and in ref 4 to derive order parameters from experimental data, we will only show in the present paper the relevant equations used, referring to ref 4 for a more complete theoretical treatment.

* To whom correspondence should be addressed.
† Università di Pisa.
‡ Scuola Normale Superiore.
§ Jagiellonian University.
|| Polish Academy of Sciences.
⊥ Military University of Technology.

10.1021/jp800378g CCC: $40.75
Published on Web 07/23/2008

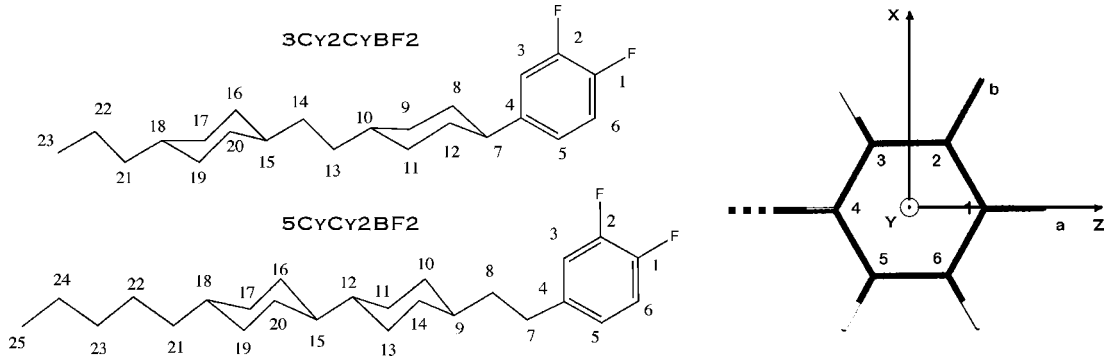

Figure 1. Molecular structures and numbering of carbon nuclei of the two fluorinated liquid crystals **3Cy2CyBF2** and **5CyCy2BF2**.

Optical, dielectric, and ^{13}C-NMR techniques provide different relationships between the measured quantities and the orientational order parameters, which, in general, are defined in molecular frames depending on the technique. The different molecular frames and degree of approximation used for getting the order parameters from the experimental quantities can both be reasons of apparent disagreement among the results obtained from the different techniques.[4–6]

The optical birefringence, $\Delta n = n_e - n_0$ (the difference between the extraordinary and ordinary refractive indices), of the nematic phase is one of the basic properties that decide about the application of LC materials in the display technology. At the same time, Δn yields information on the ordering of molecules in the N phase because it arises from the anisotropy of the polarizability tensor of the molecules and is always positive in the case of elongated shapes of molecules. The dielectric anisotropy of the N phase depends on the position and direction of the dipole moment with respect to the principal axis of the molecule (the lowest inertia moment axis), and on the order parameter. In the case of strongly polar molecules with dominating longitudinal component of the dipole moment, the order parameter is exceptionally simply related to the dielectric anisotropy which will be explored in the present study.

Local orientational order parameters in liquid crystals can be obtained from NMR exploiting either different anisotropic interactions (e.g., quadrupolar, dipolar, chemical shift) or different nuclei.[7–9] ^{1}H-NMR and ^{2}H-NMR have been particularly used for this purpose, even if both nuclei present some drawbacks: the first is severely limited by the big number of coupled protons usually present in the molecule, while deuterium NMR requires a synthetic stage for selective isotopic labeling. ^{13}C-NMR can be applied by exploiting the isotopic natural abundance,[10] even if the obtainment of order parameters is often more complex than for ^{2}H-NMR for several reasons. Scarce spectral resolution and/or non trivial signal assignment can complicate the ^{13}C-NMR analysis. Moreover, the assumptions usually performed in linking the experimental observables (either anisotropic chemical shifts or ^{13}C-^{1}H dipolar couplings) to the order parameters can be quite rough. In fact, the analysis of ^{13}C chemical shift anisotropies requires the knowledge of the ^{13}C shielding tensors principal components and their orientation respect to a molecular frame, which usually cannot be experimentally determined.[10] On the other hand, the measurement of ^{13}C-^{1}H dipolar couplings can be performed through 2D SLF experiments, which not only are time-consuming, but also require a very good spectral resolution and a reliable determination of the scaling factor f, depending upon the ^{1}H-^{1}H homonuclear dipolar decoupling sequence used.[10] Orientational order of fluorinated liquid crystals has been already studied by NMR exploiting different nuclei and/or techniques.[4,11–15] In particular, the presence of a few ^{19}F nuclei in the molecule gives rise to ^{13}C-^{19}F couplings, which can be directly extracted from monodimensional ^{13}C spectra, provided that a sufficiently good spectral resolution is achieved. However, it has been shown[4] that some complications arise in the ^{13}C-^{19}F couplings analysis, mainly due to the difficulty in separating the contributions of the scalar and dipolar couplings to the ^{13}C-^{19}F splittings experimentally determined from ^{13}C spectra.

In the present work, the good resolution obtained in static ^{13}C spectra allowed accurate ^{13}C-^{19}F splittings and anisotropic chemical shifts to be measured for all the carbons of the rigid aromatic moiety. The ^{13}C-^{19}F splittings have been analyzed to get orientational order parameters using either theoretical or empirical approximations for anisotropic scalar coupling, vibrational corrections, etc., already tested in a previous work;[4] moreover, molecular structural parameters computed by DFT methods were used. The orientational order parameters were also independently obtained by fitting all the experimental ^{13}C chemical shift anisotropies of the aromatic carbons, making use of ^{13}C shielding tensors calculated by DFT methods.

2. Experimental Section

2.1. Samples. The chemical structures of the two fluorinated liquid crystals (trans,trans) 1,2-difluoro-4-(4-(4-propylcyclohexyl)cyclohexyl)benzene [Cr-34.8°C−N-103.2°C−I] and (trans,trans) 1,2-difluoro-4-(4-(4-pentylcyclohexyl)cyclohexylethyl)benzene [Cr-25°C-SmB-73.3°C−N-121.3°C−I] are shown in Figure 1. These substances were synthsised in the Institute of Chemistry, Military University of Technology, Warsaw, Poland.

2.2. Optical and Dielectric Measurements. The optical birefringence $\Delta n = n_e - n_0$ in the N phase of **3Cy2CyBF2** and **5CyCy2BF2** was measured by the method described in ref 16. A glass plate and a convex lens composed a sample cell having variable thickness. It was placed between crossed polarizers on a microscopic stage equipped with a heater allowing stabilization of the temperature with accuracy ±0.2 K. In this arrangement, a system of circular interference fringes was observed. From the diameters of fringes the optical birefringence Δn can be calculated. All the measurements were performed by decreasing the temperature from the isotropic to the nematic phase (and also to the smectic B phase in the case of **5CyCy2BF2**). The static dielectric permittivity components, $\epsilon_\parallel$ and $\epsilon_\perp$, in the nematic phase were measured by means of an impedance analyzer, HP 4192A, using a gold-covered parallel plate capacitor ($C \sim 50$ pF). The alignments of the samples, **E** || **B** and **E** ⊥ **B** (**E** is the measuring field), were achieved by a magnetic field **B** of 0.8 T. The thickness of the sample was 0.7 mm. The temperature

TABLE 1: Dipole Moments μ and Its Components Obtained by Different Methods[a]

	3Cy2CyBF2				5CyCy2BF2			
method	μ (D)	μ_z (D)	μ_x (D)	μ_y (D)	μ (D)	μ_z (D)	μ_x (D)	μ_y (D)
SE	3.103	−2.781	−1.372	0.087	3.026	−2.865	−0.971	−0.081
QM	2.812	−2.672	−0.8767	−0.025	2.945	−2.605	−1.368	−0.118

[a] MOPAC calculations (semi-empirical, SE),[20] DFT method (quantum mechanics calculations, QM).[19]

was stabilized within ±0.2 K. For **5CyCy2BF2**, the transition from the N to B phase was accompanied by the loss of the sample alignment and the permittivity values became close to the mean value in the N phase.

2.3. ^{13}C-NMR Measurements. Solution-state spectra were recorded, at room temperature, on a Varian Unity 300 spectrometer, operating at 75.42 MHz for ^{13}C and at 299.93 MHz for ^{1}H, dissolving the samples in $CDCl_3$. ^{13}C-NMR experiments on neat liquid crystals were carried out on a double-channel Varian Infinity Plus 400 spectrometer, working at 100.56 MHz for ^{13}C, equipped with either a 5 mm goniometric probe or a 7.5 mm CP-MAS probe. In magic angle spinning (MAS) experiments, the sample, which was put within a glass ampule fitting the ZrO_2 rotor and sealed by an epoxydic glue, was spun at a frequency of 4−6 kHz. In the case of the static experiments, performed using the goniometric probe, the NMR glass tube was directly filled with the sample. Both static and MAS experiments were acquired under high-power decoupling conditions realized by means of the SPINAL-64 pulse sequence[17] with a decoupling field of about 44 and 58 kHz, respectively. The ^{1}H 90° pulse length was 4.2−5.5 μs. The ^{1}H-^{13}C cross-polarization (CP) technique with a linear ramp[18] on the carbon channel was used in all of the cases: in the nematic phases a contact time of 4 and 10 ms for static and MAS experiments, respectively, was used; for **5CyCy2BF2** within the smectic B phase a contact time of 2 and 3 ms for static and MAS experiments was employed, respectively. For both liquid crystals, ^{13}C static and MAS spectra in the nematic phase were recorded using 64 and 180 scans, respectively, while for **5CyCy2BF2** in its smectic B phase 512−1024 scans were employed in order to obtain a satisfactory signal-to-noise ratio. Relaxation delays of 15 and 7 s were used in static and MAS experiments, respectively, in order to minimize rf-heating effects due to ^{1}H-decoupling. The samples were macroscopically aligned within the superconducting magnet by slowly cooling from the isotropic phase, and the ^{13}C-NMR spectra were recorded on cooling, allowing a 30 min temperature stabilization before acquiring the spectrum. Temperature was always controlled within 0.2 K, and different cooling rates and temperature equilibration times were applied to check the reproducibility of the different phase transition temperatures. The temperature calibration was performed for a given air flow using the known phase transition temperatures of some liquid crystals.

2.4. Calculations of Molecular Geometry and Chemical Shielding Tensors. The molecular models of the mesogens **3Cy2CyBF2** and **5CyCy2BF2** were built by GaussView 3.0 (Gaussian, Inc., Pittsburgh, PA) relatively to their complete molecular structures. The geometries of these models were optimized by Gaussian'03[19] using DFT method at the B3LYP/6−31G(d) level, in vacuo. After complete optimization of the systems, relaxed scans were executed, relative to the dihedral angle ($C_3-C_4-C_7-C_8$) with steps of 15 degree in both cases, so that the relative energy minima were optimized without constraints. The location and the components of the dipole moment, μ, have been calculated by CS Mopac Pro[20] using semiempirical AM1 method (a quantum mechanical molecular orbital method with classical empirical parametrization) and DFT method, after an optimization of the molecular geometry. The results obtained are summarized in Table 1. Geometries and carbon nuclear shielding tensors were determined, for the different conformers of the models having a high statistical weight, at the DFT level of theory using the B3LYP/6−31G(d)[21] and MPW1PW91/6−311+G(d,p)[22] combination of hybrid functional and basis set, respectively. The complete shielding tensors for each carbon nucleus were obtained by means of quantum-mechanical calculations, by using the method of gauge-including atomic orbitals (GIAO)[23] implemented in Gaussian'03.[19] The chemical shift tensors were obtained by referring the absolute chemical shielding tensors obtained by DFT to the absolute shielding of TMS (185.97 ppm), which was calculated at the same level of theory of the models.

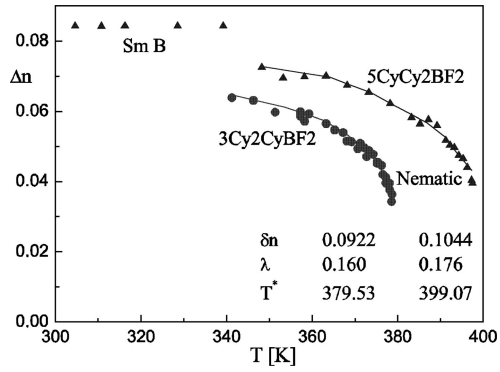

Figure 2. Optical birefringence vs temperature collected for the nematic phase of **3Cy2CyBF2** and for the nematic and smectic B phase of **5CyCy2BF2**. The lines are fits to eq 1 giving the parameters shown in the inset.

3. Results

3.1. Optical Results. The optical birefringence $\Delta n = n_e - n_0$ (the difference between the extraordinary and ordinary refractive indices) was measured throughout the liquid crystalline ranges of **3Cy2CyBF2** and **5CyCy2BF2**. The experimental data are shown in Figure 2. The temperature dependence of Δn in the N phase was fitted to the form

$$\Delta n = \delta n\left(1 - \frac{T}{T^*}\right)^{\lambda} \quad (1)$$

where T is the absolute temperature and T^*, δn, and λ are fitting parameters. This procedure is equivalent to the extrapolation of Δn to the temperature of absolute zero. Assuming that at this temperature the order parameter $S = 1$, we can calculate the order parameter as:

$$S(T) = \frac{\Delta n(T)}{\delta n} \quad (2)$$

The δn value determined for the N phase of **5CyCy2BF2** was also used for calculation of the order parameter in the B

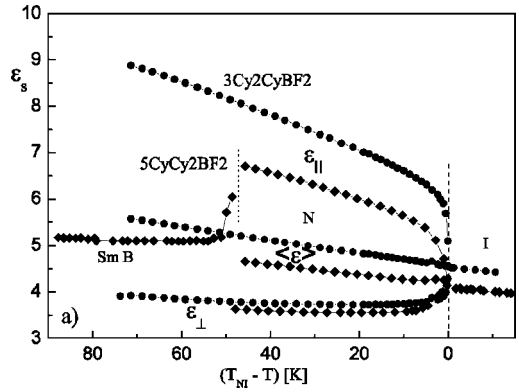

Figure 3. Static dielectric permittivity components vs shifted temperature in the nematic phase of **3Cy2CyBF2** and in the nematic and smectic B phases of **5CyCy2BF2**.

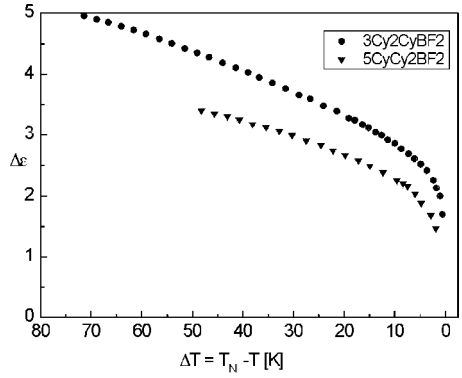

Figure 4. Dielectric anisotropy $\Delta\epsilon = \epsilon_{||} - \epsilon_\perp$ vs shifted temperature in the nematic phase of the two substances.

phase. The order parameters determined in the described way for both substances are shown in Figures 13 and 14.

3.2. Dielectric Results. The static permittivity components: $\epsilon_{||}$, $\epsilon_\perp$ and the mean value $\langle\epsilon\rangle = (\epsilon_{||}+2\epsilon_\perp)/3$, are shown in Figure 3, whereas the dielectric anisotropy $\Delta\epsilon = \epsilon_{||} - \epsilon_\perp$ is presented in Figure 4. Taking into account the different molecular structures of **3Cy2CyBF2** and **5CyCy2BF2**, the differences observed in their measured dielectric parameters should be ascribed to the position of the CH_2CH_2 bridging group (in one case between the phenyl and the cyclohexyl groups, in the other case between the two cyclohexyl groups), rather than to the different alkyl chain length, as it will be better discussed in a future work. Both compounds have the same polar part: phenyl ring with two fluorine atoms attached at the para and ortho positions that gives the dipole moment of $\mu \sim 2.2$ D. The polarity of the rest of the molecule is difficult to estimate on the basis of accessible literature data.[24] However, the results of calculations presented in Table 1 show that the real dipole moment should be distinctly larger than the above-mentioned value. The time domain spectroscopy (TDS)[25] measurements were performed for both substances in the isotropic phase, which allowed us to separate the relaxation processes connected with the molecular rotations around the principal inertia axes. The dielectric increments corresponding to both processes enabled the calculation of the β angles between the dipole moment μ and the long molecular axis.[26] The values so obtained are 28.5° for **3Cy2CyBF2**, and 43.7° for **5CyCy2BF2**.

According to Maier and Meier,[27] the dielectric anisotropy is given by

$$\Delta\epsilon = \epsilon_{||} - \epsilon_\perp = \epsilon_0^{-1} N_0 h F \left[\Delta\alpha - F\frac{\mu^2}{2k_B T}(1 - 3\cos^2\beta)\right] S \quad (3)$$

$\Delta\alpha$ is the anisotropy of the molecular polarizability, ϵ_0 is the permittivity of free space, and N_0 is the number density ($= N_A\rho/M$, M, molar mass, ρ, density, and N_A, Avogadro number). The local field factors h and F are dependent upon the mean dielectric permittivity $\langle\epsilon\rangle = (\epsilon_{||} + 2\epsilon_\perp)/3$, thus the anisotropy of the permittivity is ignored. Despite those simplifications, eq 3 is commonly used for discussion of the experimental results.[4,28–32] Equation 3 is especially useful for determining the order parameter of strongly polar compounds (having large dielectric anisotropy) because in that case the dipolar polarizability μ^2/k_BT dominates in square brackets of eq 3 and $\Delta\alpha$ can also be ignored. So, the following simplified relation between $\Delta\epsilon$ and S can be applied

$$S(T) \propto \frac{T\Delta\epsilon(T)}{hF^2} \quad (4)$$

(Density of the substances studied is not known but the expansion coefficient in the nematic phase is $\sim 10^{-4}$ K $^{-1}$, and the temperature dependence of N_0 can be ignored in relation to the change of $\Delta\epsilon(T)$). For both substances studied, the values of the polarizability anisotropy were not determined experimentally as yet. Taking into account small birefringence values (Figure 2), being close to those observed in the case of similar substances,[4,33] one can estimate $\Delta\alpha \approx 10$ Å^3.

The values of the local field parameters, calculated from the permittivity data presented in Figure 3, are $h \sim 1.36$ and 1.35, $F \sim 1.41$ and 1.38 for **3Cy2CyBF2** and **5CyCy2BF2**, respectively, and they slightly increase with decreasing temperature. Taking into account the above data, the relation $\Delta\alpha \ll F\mu^2/2k_BT$ is valid and the relation (eq 4) can be used. Because the absolute value of the order parameter cannot be obtained in this way, the trend of the order parameter with temperature was assumed to follow the Haller[34] relation

$$S(T) = S_0(\Delta T)^\gamma \quad (5)$$

with $S_0 = 1/T_{NI}^\gamma$, where $\Delta T = T_{NI} - T$ is the shifted temperature. The order parameter values derived in this way are shown in Figures 13 and 14 together with other results.

3.3. ^{13}C-NMR Results. ***3.3.1. Spectral Assignment and Spectral Parameters Determination.*** The dipolar splittings and the anisotropic chemical shifts in difluorinated liquid crystals can be usually directly measured from ^{13}C-NMR static spectra, provided to have a sufficient spectral resolution (requiring efficient proton decoupling schemes), and to be able to assign all the signals present in the spectra recorded at the different temperatures within the mesophases. The last requirement is often nontrivial due to the dependence of the observed chemical shifts from both the chemical shielding tensor components and the order parameters, usually making difficult the correlation between the chemical shift values observed in the mesophase (δ^{obs}) and the isotropic ones (δ^{iso}). Here, we managed to fully assign all the ^{13}C-NMR static spectra of both the molecules investigated by looking at the magnitude of both the observed dipolar splittings and chemical shift, as well as at their trends with temperature. Moreover, the individual trends of δ_i^{obs} could be safely extrapolated to a virtual temperature, higher than T_{NI}, at which the order parameters would vanish in the overheated nematic phase and where the extrapolated δ_i^{obs} value ideally

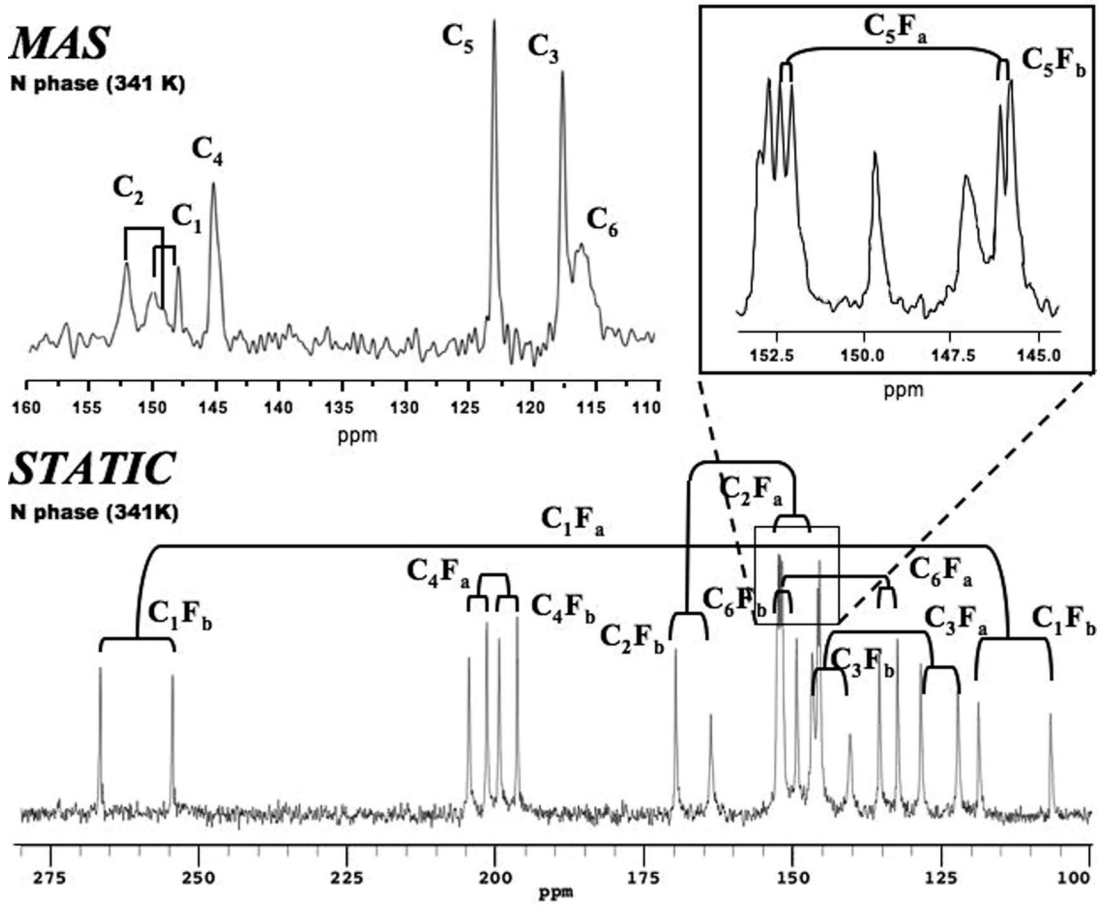

Figure 5. Expansion of the aromatic region of ^{13}C-NMR CP-MAS and CP static spectra of **3Cy2CyBF2**, recorded with the SPINAL-64[17] decoupling technique at 341 K. The assignment of the spectra refers to carbon numbering shown in Figure 1.

matches the corresponding δ_i^{iso} value.[4] For these reasons, a ^{13}C-NMR solution state and MAS study was preliminarly performed.

The assignment of the solution state ^{13}C spectra (not shown) for both **3Cy2CyBF2** and **5CyCy2BF2** was carried out on the basis of ^{13}C DEPT, ^{1}H-^{13}C 2D-HETCOR, and ^{1}H spectra, as well as of computed GIAO-DFT isotropic chemical shift values. The values of ^{13}C isotropic chemical shifts obtained from solution state spectra are reported in Table 2, where they are compared with those either obtained from the MAS experiments recorded in the mesophases, or determined by means of in vacuo DFT-GIAO calculations. The assignment of ^{13}C resonances was finally checked by comparison with that previously performed for a similar difluorinated liquid crystal, **3CyCyBF2**.[4] Solution state spectra were also useful for determining the absolute values of the ^{13}C-^{19}F isotropic scalar coupling constants (J_{ij}^{iso}) for the aromatic carbons (see Tables 3 and 4). The signs of these coupling constants were assigned according to the literature.[35]

From the ^{13}C CP-MAS spectra (see Figures 5 and 6), it was found that the values of the isotropic chemical shifts of each carbon nucleus experience only small changes with temperature within the nematic ranges (up to a maximum of 50 Hz, less than the experimental line width), while in the smectic B phase of **5CyCy2BF2** a systematic decrease of δ_{MAS}^{iso} with decreasing temperature was detected, even if the effect is relatively small (Supporting Information). The average values of the ^{13}C MAS chemical shifts, reported in Table 2, are in good agreement with both calculated and solution-state chemical shifts: the differences

TABLE 2: Isotropic, MAS, and Theoretical Chemical Shifts for Both Fluorinated Liquid Crystals Studied in This Work[a]

	3Cy2CyBF2			5CyCy2BF2		
C_n	δ_{GIAO} (ppm)	$\delta_{isotropic}$ (ppm)	δ_{MAS} (ppm)	δ_{GIAO} (ppm)	$\delta_{isotropic}$ (ppm)	δ_{MAS} (ppm)
1	149.72	148.80	149.3	151.65	148.74	149.4
2	151.59	150.46	150.8	153.35	150.55	150.9
3	114.69	116.96	117.2	117.06	117.11	117.4
4	145.88	145.12	145.2	141.30	140.34	140.4
5	123.04	122.73	122.8	123.11	124.21	124.2
6	116.62	115.64	115.8	116.82	117.01	116.3

[a] The isotropic chemical shifts were measured from solution state spectra recorded in $CDCl_3$; MAS chemical shift values were obtained as average over the different temperatures in the whole mesomorphic range; the theoretical chemical shifts were computed by DFT calculations using the GIAO method[23] in Gaussian '03.[19]

for most of the aromatic signals are less than 1 ppm and they never exceed 3 ppm.

^{13}C CP spectra of both **3Cy2CyBF2** and **5CyCy2BF2** were also recorded under static conditions throughout the mesomorphic ranges of both the samples investigated. In Figures 5 and 6, expansions of the aromatic regions of these spectra for each sample are reported, together with the corresponding signal assignment. The difference between static and MAS spectra is due to the effects of the anisotropic interactions, and, in particular, of the ^{13}C-^{19}F dipolar and scalar couplings, and the anisotropic component of chemical shift (δ^{aniso}). The dipolar and scalar couplings split each ^{13}C aromatic signal in one doublet for each ^{19}F nucleus present in the ring (see

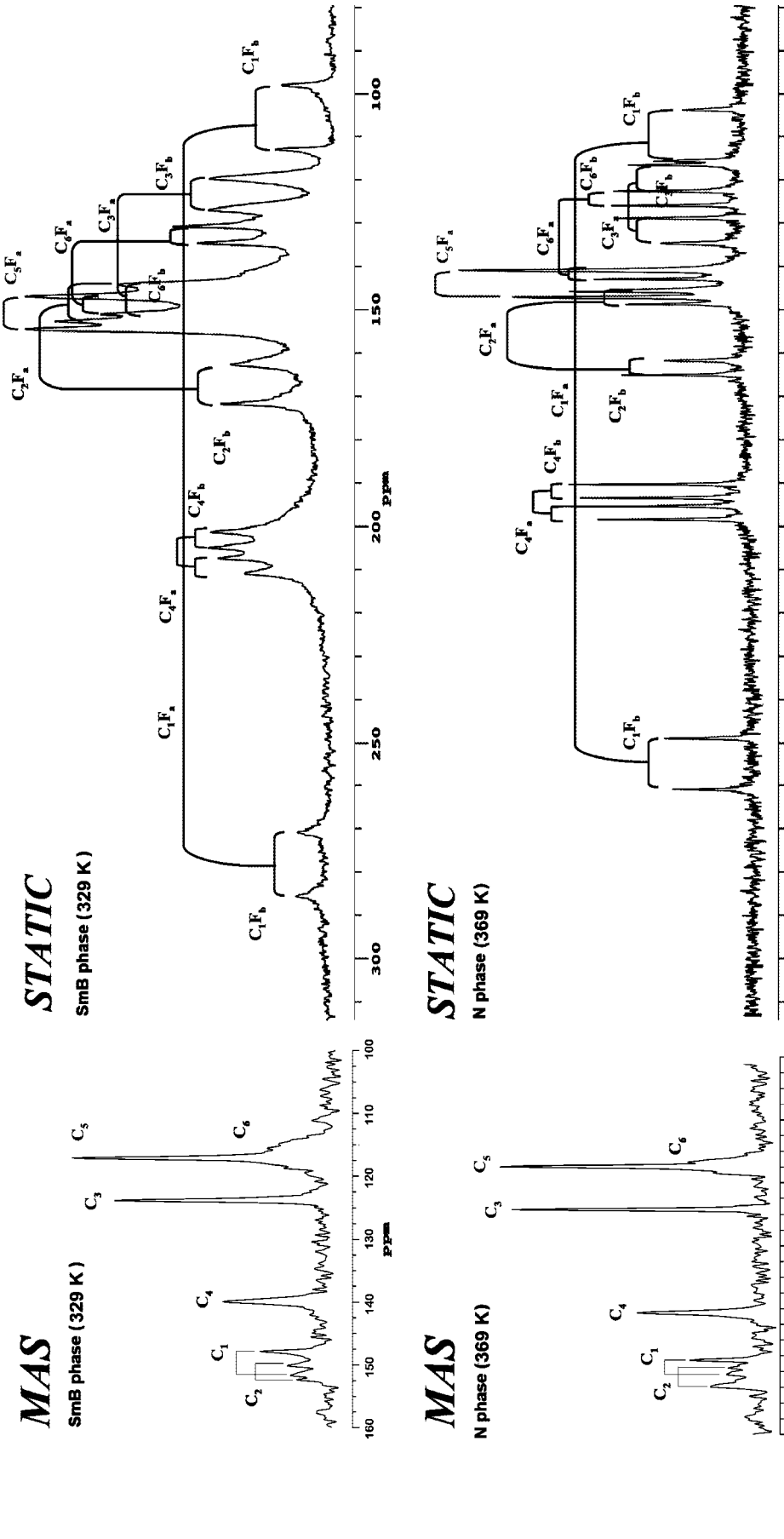

Figure 6. Expansion of the aromatic region of ^{13}C-NMR CP-MAS and CP static spectra of **5CyCy2BF2**, recorded with the SPINAL-64[17] decoupling technique at 369 K (Nematic phase) and at 329 K (Smectic B phase). The assignment of the spectra refers to carbon numbering shown in Figure 1.

TABLE 3: Geometrical Parameters: $F_{a/b}$-C_n Distances, $\vartheta_{\xi n}$ Angles between the Cartesian Axis ξ and the Vector Connecting Fluorine (a/b) with Carbon n, and Molecular Parameters (Experimental J^{iso} Measured by ^{13}C-NMR of the Mesogen Dissolved in $CDCl_3$, ΔJ, $J_{xx} - J_{yy}$, and J_{xz} Taken from Reference 37 and D^h Contribution Percentage Estimated from Reference 37) Relative to the Aromatic Fragment of 3Cy2CyBF2

F_i	C_n	r_{ij} (Å)	ϑ_{zn} (°)	ϑ_{xn} (°)	ϑ_{yn} (°)	J^{iso} (Hz)	ΔJ (Hz)	$J_{xx} - J_{yy}$ (Hz)	J_{xz} (Hz)	D^h (%)
a	1	1.346	1.26	−88.74	90.00	−244.8	400.0	13.0		−2.57
a	2	2.361	−29.73	−119.73	90.00	12.0				−0.99
a	3	3.635	−18.92	−108.92	90.00					−0.35
a	4	4.155	0.41	−89.59	90.00	5.3				−0.14
a	5	3.642	19.72	−70.28	90.00	5.8				−0.35
a	6	2.377	31.28	−58.72	90.00	16.7				−0.99
b	1	2.361	90.54	−0.54	90.00	12.6				−0.99
b	2	1.346	59.41	−30.59	90.00	−246.8	−45.12	458.12	257.0	−2.57
b	3	2.370	29.09	−60.91	90.00	16.6				−0.99
b	4	3.652	40.26	−49.74	90.00	4.1				−0.35
b	5	4.126	60.12	−29.88	90.00	3.4				−0.14
b	6	3.626	79.45	−10.55	90.00					−0.35

TABLE 4: Geometrical Parameters: $F_{a/b}$-C_n Distances, $\vartheta_{\xi n}$ Angles between the Cartesian Axis ξ and the Vector Connecting Fluorine (a/b) with Carbon n, and Molecular Parameter J^{iso}, Measured by ^{13}C-NMR of the Mesogen Dissolved in $CDCl_3$[a]

F_i	C_n	r_{ij} (Å)	ϑ_{zn} (°)	ϑ_{xn} (°)	ϑ_{yn} (°)	J^{iso} (Hz)
a	1	1.346	1.18	−88.82	90.00	−243.5
a	2	2.361	−29.60	−119.40	90.00	12.1
a	3	3.635	−18.73	−108.73	90.00	
a	4	4.151	0.41	−89.59	90.00	5.6
a	5	3.641	19.92	−70.08	90.00	5.9
a	6	2.377	31.48	−58.52	90.00	16.3
b	1	2.364	89.34	−0.66	90.00	12.7
b	2	1.347	59.64	−30.46	90.00	−245.7
b	3	2.371	29.32	−60.68	90.00	16.1
b	4	3.651	39.91	−50.09	90.00	3.8
b	5	4.116	60.14	−29.86	90.00	3.4
b	6	3.628	79.65	−10.35	90.00	

[a] The parameters ΔJ, $J_{xx} - J_{yy}$, *and* J_{xz} and D^h relative to the aromatic fragment of **5CyCy2BF2** are the same used for the **3Cy2CyBF2** and reported in Table 3.

eq 6), with splittings, $\Delta\nu$, ranging from tens to thousands of Hertz. Since in **3Cy2CyBF2** and **5CyCy2BF2** two inequivalent ^{19}F nuclei are in the aromatic ring, each aromatic carbon is split into a quartet. The chemical shift anisotropy gives rise to a high-frequency shift of the center of the multiplets (δ^{obs}) by up to 50 ppm. The strong dependence of splittings and chemical shifts on the order parameters causes the regular changes experienced by the spectra with temperature (see Figures 7, 11 and 8, 12).

The assignment of the static spectra was performed on the basis of the magnitude of the observed splittings and chemical shift anisotropies, and of the trends of both the individual signals and δ^{exp} with temperature (see Figures 7, 8 and 11, 12). All the assignments were validated a posteriori by the global analysis of the splittings $\Delta\nu$ performed for determining the order parameters. In fact, the predicted values of dipolar splittings (see Figures 9 and 10, solid lines) and chemical shift anisotropies (see Figures 11 and 12, solid lines) for each aromatic carbons are in very good agreement with the experimental ones. It must be noticed that the relative values of the splittings $\Delta\nu$ are strictly constrained by the molecular geometry, and therefore an incorrect assignment of the signals would give rise to a noticeable difference between calculated and experimental splittings for the mistakenly assigned carbon nuclei. From each splitting $\Delta\nu_{ij}$ a value of D_{ij}^{exp} was obtained from the equation:

$$\Delta\nu_{ij} = 2D_{ij}^{exp} + J_{ij}^{iso} \quad (6)$$

using the values of J_{ij} determined from solution spectra and reported in Tables 3 and 4.

3.3.2. Determination of Order Parameters. To obtain the order parameters relative to the aromatic fragments of the two fluorinated mesogens, we performed a global analysis of the D_{ij}^{exp} values for the six carbons of the aromatic ring at all temperatures, using the following equations:[4]

$$D_{ij}^{exp} = D_{ij}^{eq} + D_{ij}^{h} + D_{ij}^{ah} + D_{ij}^{d} + \frac{1}{2}J_{ij}^{aniso} \quad (7)$$

D_{ij}^{eq} is the dipole−dipole coupling corresponding to the equilibrium structure of the molecule, D_{ij}^{h} is the contribution from the harmonic vibrations, D_{ij}^{ah} arises from the anharmonicity of the vibrational potential and D_{ij}^{d} is the deformation contribution of the molecular structure due to anisotropic forces of the solvent molecules.[36] The terms D_{ij}^{ah} and D_{ij}^{d} are usually estimated

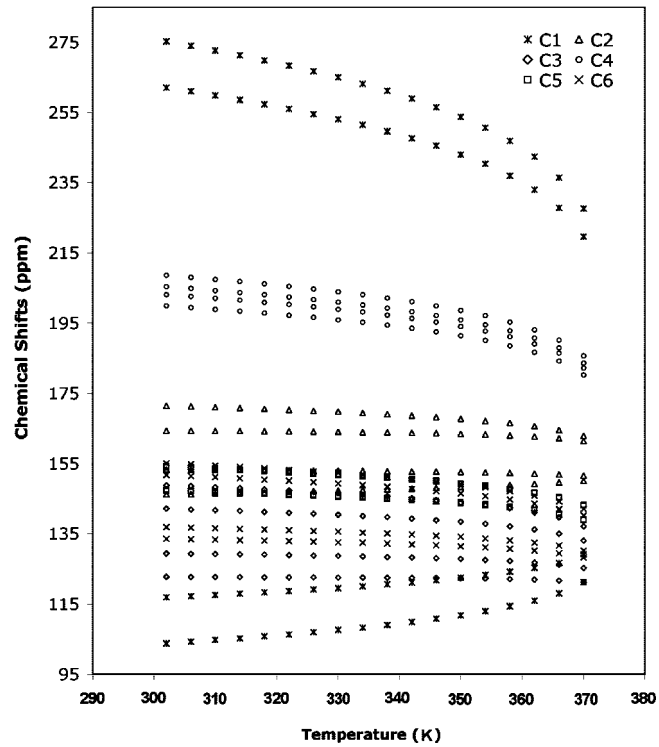

Figure 7. Trends vs temperature of ^{13}C static chemical shifts for each distinguishable peak in the spectral aromatic region of **3Cy2CyBF2**.

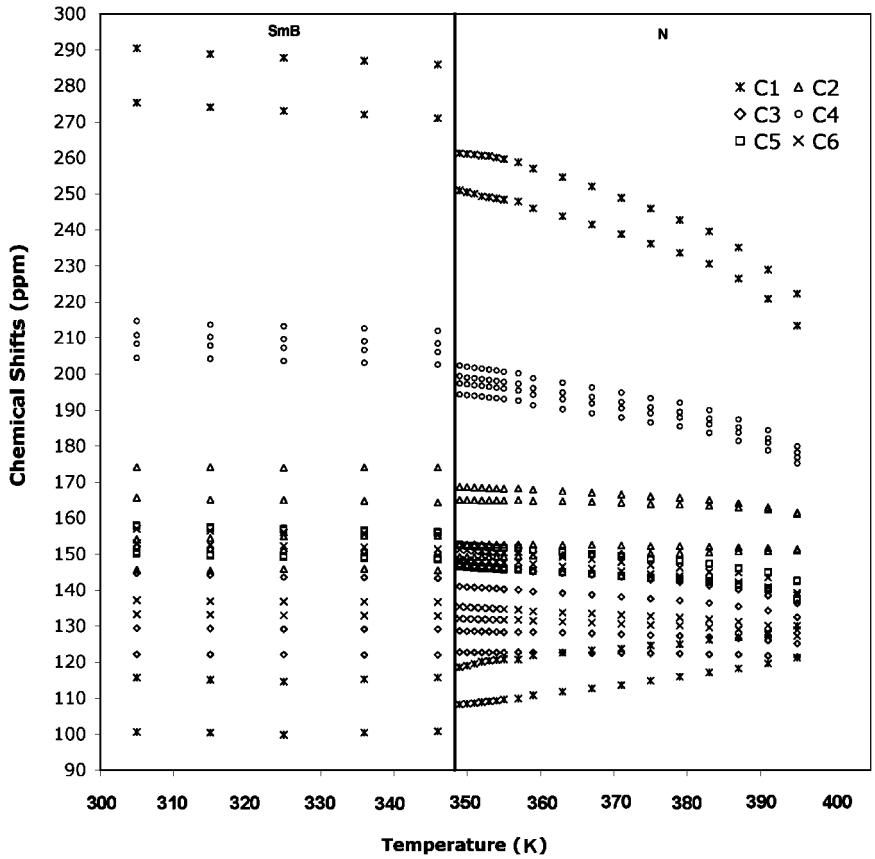

Figure 8. Trends vs temperature of ^{13}C static chemical shifts for each distinguishable peak in the spectral aromatic region of **5CyCy2BF2**.

to be smaller than the experimental error on the measured splittings, and therefore they can be safely neglected.[37]

The "equilibrium" dipole-dipole coupling, D_{ij}^{eq}, is related to the order parameter S_{ij} of the internuclear ij direction through the equation

$$D_{ij}^{eq} = -K_{ij} \cdot \frac{S_{ij}}{r_{ij}^3} \tag{8}$$

where r_{ij} is the equilibrium distance between the two nuclei i and j, and K_{ij} is the dipolar constant

$$K_{ij} = \frac{\mu_0 \hbar \gamma_i \gamma_j}{8\pi^2} \tag{9}$$

The local order parameter S_{ij} can be in general expressed in terms of the components of the Saupe matrix relative to a convenient (x,y,z) molecular frame:

$$S_{ij} = \frac{1}{2}S_{zz}(3\cos^2\theta_{ij,z} - 1) + \frac{1}{2}(S_{xx} - S_{yy})(\cos^2\theta_{ij,x} - \cos^2\theta_{ij,y}) + 2S_{xz}\cos\theta_{ij,x}\cos\theta_{ij,z} + 2S_{xy}\cos\theta_{ij,x}\cos\theta_{ij,y} + 2S_{yz}\cos\theta_{ij,y}\cos\theta_{ij,z} \tag{10}$$

where $\theta_{ij,\epsilon}$ is the angle between the ij direction and the ϵ axis of the molecular frame.

D_{ij}^{h} can be considered a correction of D_{ij}^{eq}, non-negligible only for spatially close couples of nuclei, because of its $1/r_{ij}^5$ dependence.[38] The D_{ij}^{h} values can be roughly estimated in analogy with those determined for molecules of similar structure and orientation.[36]

J_{ij}^{aniso} can be expressed in terms of the order parameters and of the tensorial components $J_{ij,\epsilon\tau}$ relative to the molecule-fixed coordinate system (x,y,z)

$$J_{ij}^{aniso} = \frac{2}{3}\Big[\Delta J_{ij} S_{zz} + \frac{1}{2}(J_{ij,xx} - J_{ij,yy})(S_{xx} - S_{yy}) + 2J_{ij,xy}S_{xy} + 2J_{ij,xz}S_{xz} + 2J_{ij,yz}S_{yz}\Big] \tag{11}$$

The quantity

$$\Delta J_{ij} = J_{ij,zz} - \frac{1}{2}(J_{ij,xx} + J_{ij,yy}) \tag{12}$$

defines the anisotropy of **J** with respect to the molecular z axis for the ij couple of nuclei.

The internuclear distances and the angles required to use eqs 8 and 10 were determined by DFT calculations. The energetic barriers for the rotation of the aromatic fragments about their para axes for both fluorinated mesogens are relatively small: 2.2 and 1.8 kcal/mol for **3Cy2CyBF2** and **5CyCy2BF2**, respectively, indicating in both cases the occurrence of an almost free rotation. The bond lengths and angles calculated for minimum energy conformations of **3Cy2CyBF2** and **5CyCy2BF2** are reported in Tables 3 and 4. The geometrical parameters calculated for the various conformers are substantially equal to those calculated for the minimum energy conformer, bonds, and angles differing by less than 0.01 Å and 0.01°, respectively.

Fixing the axes frames as indicated in Figure 1 for both liquid crystals, the order parameters that can be determined are S_{zz}, $(S_{xx} - S_{yy})$ and S_{xz}. In fact, as always happens dealing with sets of couplings between nuclei of an aromatic ring, S_{xy} and S_{yz} cannot be determined since in eq 10 they multiply vanishing geometrical factors.

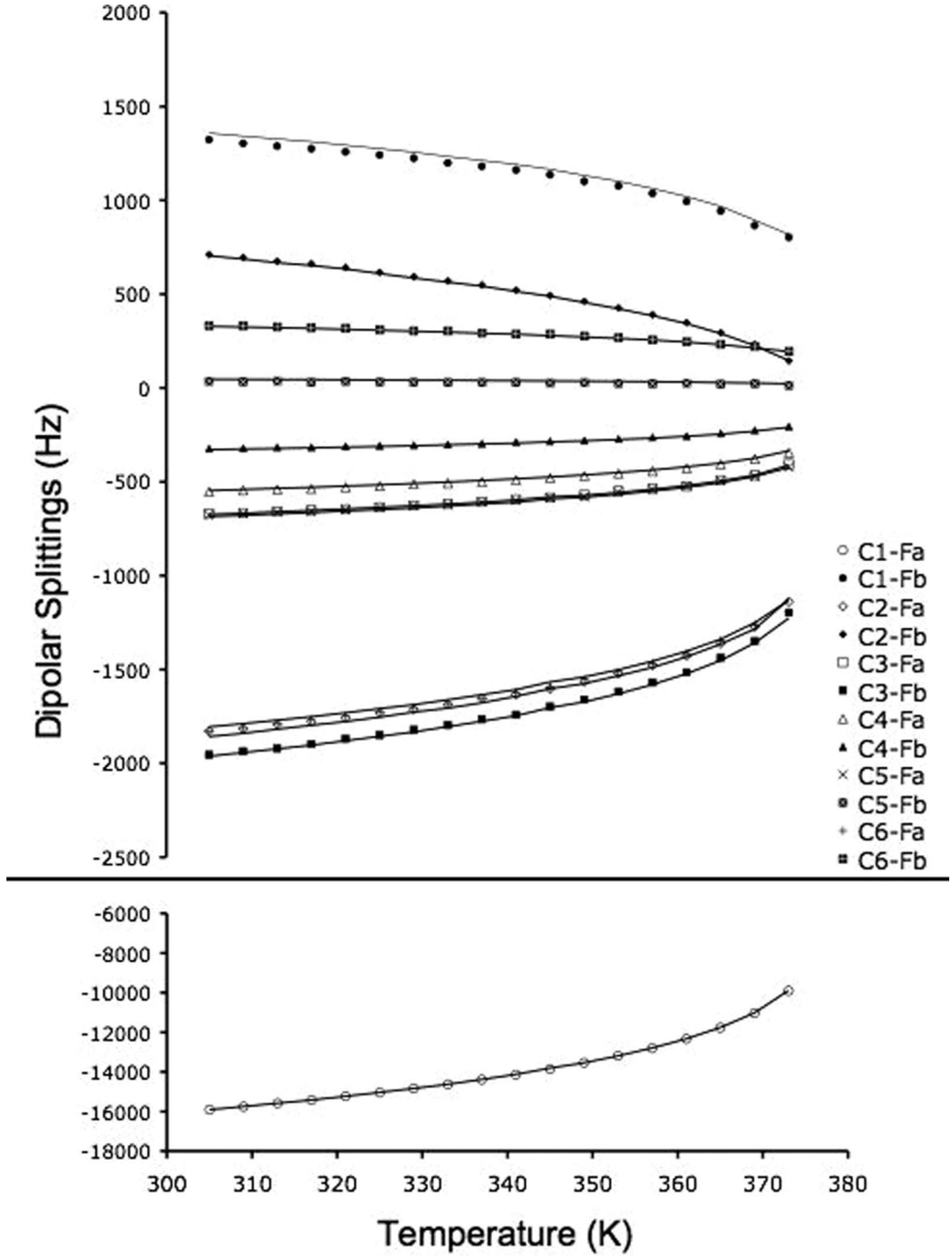

Figure 9. Trends of the experimental (symbols) and calculated (solid lines) dipolar splittings, D_{ij}^{exp}, for each aromatic ^{13}C-^{19}F couple of **3Cy2CyBF2** on the whole temperature range investigated.

To estimate the contributions of the terms D^{ah}, D^{h}, D^{d} and J^{aniso} to D^{exp} (see eq 7), as already done for the determination of the orientational order parameters for **3CyHeBF** and **3CyCyBF2**,[4] we exploited the results reported for *para*-difluorobenzene in refs 36 and 37, where the authors performed very accurate determinations of all the terms by means of a combined theoretical and experimental approach. In particular, the terms D^{ah} and D^{d} were predicted to be very small, and therefore could be safely neglected in the analysis. The fitting of the D_{ij}^{exp} values to determine the order parameters was performed taking into account both the contributions of D^{h} and J^{aniso}, in agreement with the procedure followed in a previous study, which was found to give good results.[4]

The term D^{h} was considered as a correction to be applied to each D_{ij}^{exp} value before performing the global analysis. Its contribution percentage to D^{exp} was estimated for each ^{13}C-^{19}F dipolar coupling from the ratio D^{h}/D^{eq} and is reported in Tables 3 and 4.[37]

The term J^{aniso} could be included in the global analysis of the D_{ij}^{exp} values by means of equation 11, deriving an estimate of ΔJ and $J_{xx} - J_{yy}$ from ref 36. The values used in the cases of **3Cy2CyBF2** and **5CyCy2BF2** are shown in Tables 3 and 4, respectively. Only the most important J^{aniso} contributions were taken into account, relative to the two couples of directly bonded ^{13}C-^{19}F nuclei. The data reported in Tables 3 and 4 for the C_2-F_b couple were obtained after applying the appropriate rotation to the J^{aniso} tensor, given in ref 36, from its principal axes system to the ring-fixed (x,y,z) one.

The agreement between experimental and calculated ^{13}C-^{19}F dipolar splittings is very good for both liquid crystals in all the

mesophasic ranges, as shown in Figures 9 and 10. The trends of S_{zz} versus temperature are reported in Figures 13 and 14 for **3Cy2CyBF2** and **5CyCy2BF2**, respectively. For **3Cy2CyBF2** the biaxiality ($S_{xx} - S_{yy}$) and the S_{xz} order parameter are about constant with temperature at values of 0.068 ± 0.005 and -0.013 ± 0.002, respectively. For **5CyCy2BF2** different trends of the ($S_{xx} - S_{yy}$) and of S_{xz} with temperature are observed for the two mesophases. The biaxiality varies with decreasing temperature from 0.042 to 0.093 ± 0.007 in the nematic phase, while it is about constant in the SmB phase (0.07 ± 0.01). The same behavior is observed for the S_{xz} order parameter, which varies with decreasing temperature from -0.02 to $+0.02 \pm 0.01$ in the nematic phase, while it is about constant in the SmB phase (-0.026 ± 0.002).

Orientational order parameters were also independently obtained for both samples from a global fitting of the anisotropic chemical shifts ($\delta_i^{\text{aniso}} = \delta_i^{\text{obs}} - \delta_i^{\text{iso}}$) measured for all the aromatic carbons, on the basis of the following equations:

$$\delta_i^{\text{aniso}} = \frac{2}{3}\Big[\Delta\delta_i S_{zz} + \frac{1}{2}(\delta_{i,xx} - \delta_{i,yy})(S_{xx} - S_{yy}) + 2\delta_{i,xy}S_{xy} + 2\delta_{i,xz}S_{xz} + 2\delta_{i,yz}S_{yz}\Big] \quad (13)$$

$\delta_{i,\epsilon\tau}$ are the component of the i-th chemical shift tensor written in the molecule-fixed coordinate system where the Saupe ordering matrix is defined. The quantity

$$\Delta\delta_i = \delta_{i,zz} - \frac{1}{2}(\delta_{i,xx} + \delta_{i,yy}) \quad (14)$$

defines the anisotropy of δ with respect to the molecular z axis.

The chemical shift tensor components, present in eq 13 and needed for the determination of order parameters, were computed by DFT methods, which were shown to give good results in mesogenic compounds,[39] and are reported in Table 5. As in the case of dipolar splittings, also for anisotropic chemical shifts the agreement between experimental and calculated values was very good, as can be seen in Figures 11 and 12. The trends of S_{zz} versus temperature are reported in Figures 13 and 14 for **3Cy2CyBF2** and **5CyCy2BF2**, respectively. For **3Cy2CyBF2** the biaxiality ($S_{xx} - S_{yy}$) and the S_{xz} order parameter are in very good agreement with those determined by ^{13}C-^{19}F dipolar couplings and their trends with temperature are constant at values of 0.071 ± 0.004 and -0.011 ± 0.002, respectively. For **5CyCy2BF2** the biaxiality varies with decreasing temperature from 0.122 to 0.165 ± 0.003 in the nematic phase, while it is about constant in the SmB phase (0.11 ± 0.01). The same behavior is observed for the S_{xz} order parameter, which varies with decreasing temperature from -0.03 to 0.04 ± 0.01 in the nematic phase, while it is about constant in the SmB phase (-0.045 ± 0.001).

4. Discussion

The four different approaches followed in this paper to derive orientational order parameters (from dielectric anisotropy, optical birefringence, ^{13}C-^{19}F dipolar couplings, and ^{13}C chemical shift anisotropy) present differences which must be discussed before comparing the results obtained. A first difference concerns the different anisotropic physical quantities measured and, consequently, the different axis frame in which the order parameters are defined. Dielectric and optical methods measure whole-molecule quantities, and therefore molecular order parameters are derived, defined in the polarizability and dielectric tensor principal axes frames, respectively. On the contrary, in NMR local properties at the sites of the nuclei investigated are measured, and the orientational order parameters so determined refer to molecular fragments (in our case to the fluorinated phenyl fragment). Another difference consists in the possibility offered by NMR of deriving order parameters independently at each temperature, although this was not the case of optical birefringence and dielectric measurements for which the assumption of a suitable model giving the trend of order parameters with temperature was necessary. Moreover, while from both NMR approaches also the orientational order biaxiality ($S_{xx} - S_{yy}$) (albeit referred to the rigid fluorinated fragment, like S_{zz}) could be derived, this was assumed negligible in both dielectric and optical data analyses, which could give the sole order parameter S_{zz}. The determination of order parameters from optical and dielectric methods required several simplifying assumptions. As previously discussed, in the case of dielectric anisotropy data it was assumed that the Maier−Meier formula (see eq 3) may be reduced to a simple relation (see eq 4), thus neglecting the temperature dependence of the density, as well as the polarizability anisotropy of the molecules; while the first assumption is well fulfilled, the second one is reliably justified only in the case of strongly polar compounds. In the case of optical studies, the local field problem was overcome by applying, for the normalization of the optical birefringence, an empirical formula proposed by Haller for polarizabilities, leading to eq 1. Differences were also present between the two NMR methods, consisting in the analysis of either ^{13}C-^{19}F dipolar couplings or ^{13}C chemical shift anisotropies. In principle, these two methods should give the same orientational order parameters, since the frame where the ordering matrix is defined is the same in the two cases. However, different experimental errors in the measurement of the NMR observables, and, most important, different assumptions and approximantions are present in the two cases, which might bring to different values of the derived S_{zz} and ($S_{xx} - S_{yy}$) quantities. On one side, the availability of a large set of ^{13}C-^{19}F couplings allowed the experimental data to be treated in a quite refined way, taking into account the empirically estimated contributions arising from the anisotropic scalar interaction and possible deformations of the geometry due to harmonic vibrations. Even though this analysis can be considered quite reliable, as extensively discussed in ref 4, the absence of a more refined vibrational analysis could be the cause of some systematic errors in the derived orientational order parameters. On the other hand, in the analysis of the chemical shift anisotropies the main error affecting the order parameters could arise from the values used for the ^{13}C chemical shielding tensors, which in our case were calculated using DFT methods in vacuo. Nevertheless, the substantial agreement of these data with those obtained from the other methods confirms the good reliability of the calculated ^{13}C nuclear shielding tensors.

All this considered, the experimental data obtained from the four methods were analyzed by suitable models giving the S_{zz} versus temperature trend, and the corresponding results compared, also resorting to suitable normalization procedures.

The dielectric and optical data were at first analyzed in the nematic phases assuming that the orientational order parameter changed with temperature according to the Haller eq 5. This equation is largely used in treating these data, even if it is incompatible with the weakly first order character of the N − I transition, as it predicts continuous decrease of S to zero approaching T_{NI}. For this reason, in fitting the experimental data the points close to T_{NI} have been ignored. The fits of the dielectric and optical data, as well as those of the NMR order parameters were very good for both the substances studied

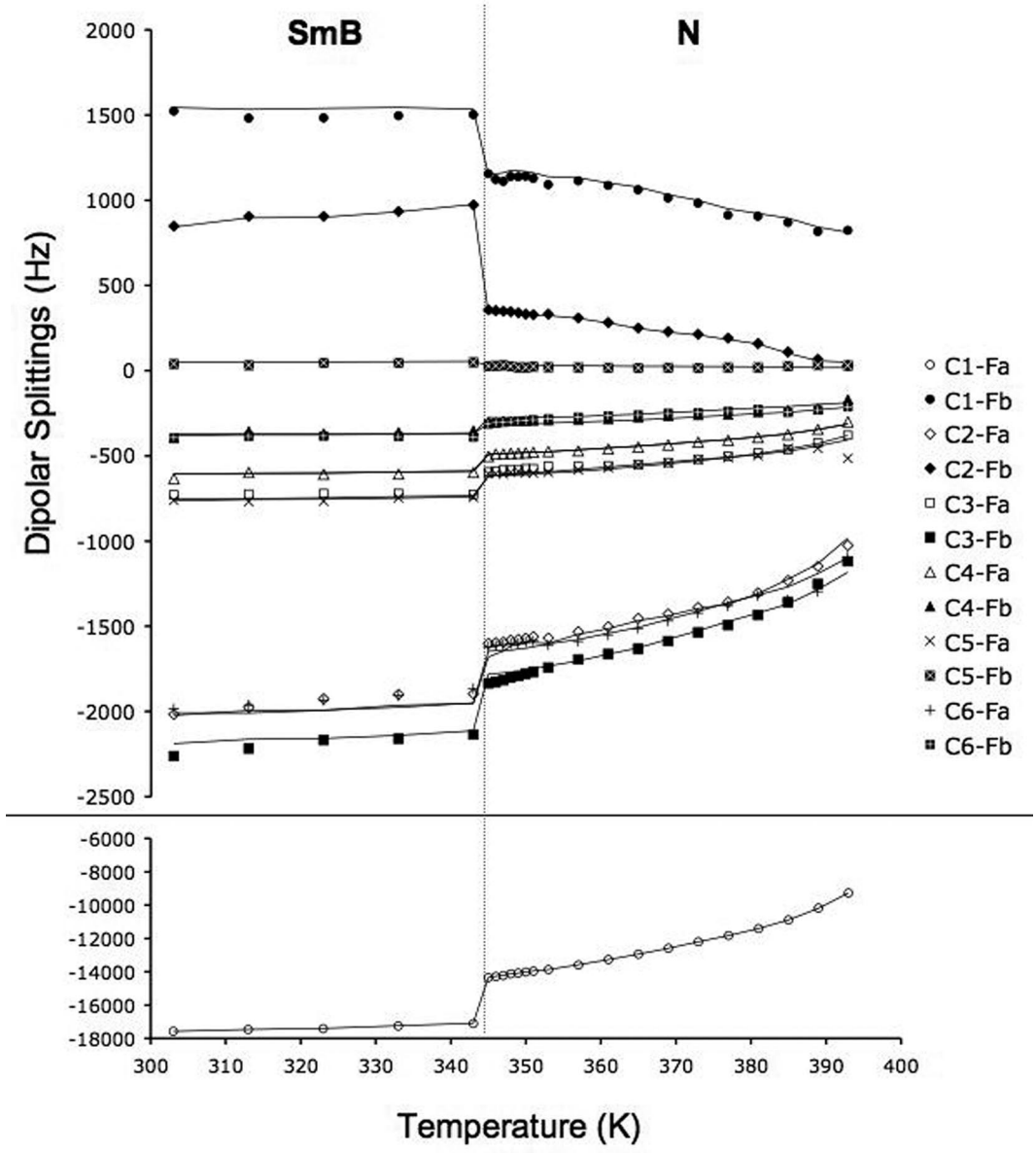

Figure 10. Trends of the experimental (symbols) and calculated (solid lines) dipolar splittings, D_{ij}^{exp}, for each aromatic ^{13}C-^{19}F couple of **5CyCy2BF2** on the whole temperature range investigated.

(Supporting Information). The same data were also fitted by the refined four-parameter equation proposed by Chirtoc et al.,[40] which is consistent with the mean-field theory for a weakly first order phase transition

$$S(T) = S^{**} + A \cdot \tau^{\eta} \quad (15)$$

with η the critical exponent ($\approx$0.25 according to the mean-field theory) and $\tau = (1\text{-}T/T^{**})$ the reduced temperature. T^{**} is the effective second order (quasi-critical or quasi-tricritical) phase transition point seen from below T_{NI} and is slightly higher than T_{NI}. With the condition $S(0) = 1$ at $T = 0$ we have $S^{**} + A = 1$. The fits of the Chirtoc et al. equation to the experimental (dielectric, optical, and NMR) data are excellent and are presented in Figures 13 and 14. The best-fitting parameters obtained (Supporting Information) roughly satisfy the relations $S^{**} + A \approx 1$ and $\eta \approx 0.25$, in agreement with the above considerations. On the contrary, the γ parameter of eq 5, which plays a role analogous to η in eq 15, was found in all cases much lower than 0.25. These results are also in agreement with those previously obtained for two different fluorinated nematogens.[4]

As it can be seen, the order parameters S_{zz} obtained from the four different methods were in very good agreement: those arising from dielectric and optical measurements were almost coincident, while the largest differences were with the order parameters obtained from ^{13}C-^{19}F dipolar couplings. Anyway, apart from a quite modest shift among the different sets of results, their trends versus temperature appeared to be quite the same in all cases, as indicated by very similar A (ranging from 0.82 to 0.88 for **3Cy2CyBF2** and from 0.81 to 0.92 for **5CyCy2BF2**) and η (0.228−0.232 for **3Cy2CyBF2** and 0.233−0.255 for **5CyCy2BF2**), and slightly different S^{**} (0.14−0.19 for **3Cy2CyBF2** and 0.11−0.19 for **5CyCy2BF2**) best-fitting values obtained for the four different sets of data. The results obtained from ^{13}C chemical shift anisotropies were chosen as reference data, which "normalize" all the other sets of data. In the case of dielectric and optical data, this normalization procedure could be indicative of the angle between the z-axes along which S_{zz} was defined in the different methods and therefore also allowed the order parameters obtained in different ways to be referred to the same molecular frame. This does not apply to the order parameters obtained from ^{13}C-^{19}F

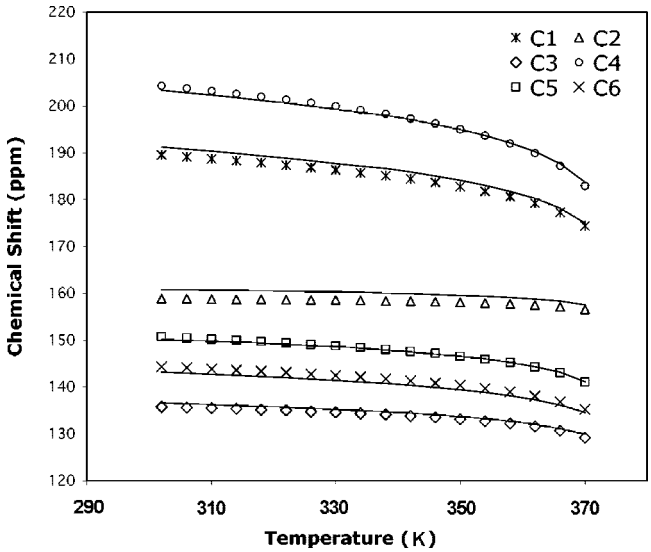

Figure 11. Trends of the experimental (symbols) chemical shifts δ_i^{obs} measured from the static spectra (as the average of the chemical shifts of the four lines of each ^{13}C quartet reported in Figure 7) and corresponding calculated values (solid lines) for each chemically distinguishable aromatic ^{13}C nucleus of **3Cy2CyBF2** on the whole temperature range investigated.

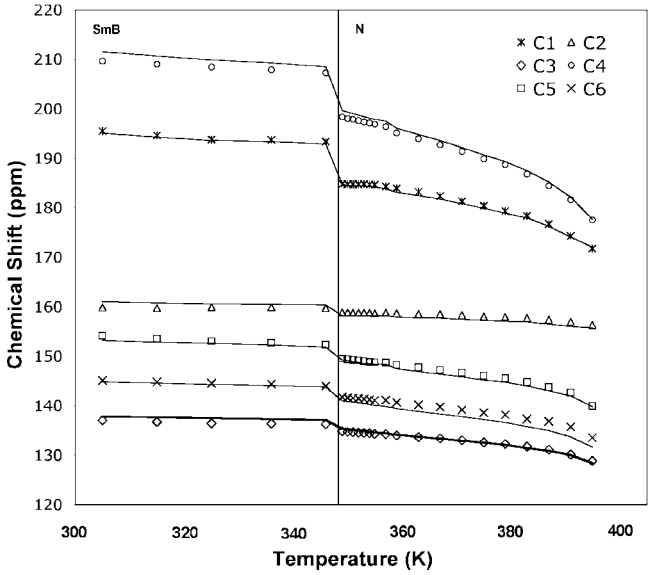

Figure 12. Trends of the experimental (symbols) chemical shifts δ_i^{obs} measured from the static spectra (as the average of the chemical shifts of the four lines of each ^{13}C quartet reported in Figure 8) and corresponding calculated values (solid lines) for each chemically distinguished aromatic ^{13}C nucleus of **5CyCy2BF2** on the whole temperature range investigated.

dipolar couplings, since in this case the *z*-axis is the para axis of the phenyl ring, as for the ^{13}C chemical shift anisotropies. Therefore, the normalization in this case would only take into account systematic errors having either an experimental or data analysis nature, as previously discussed. The "normalizing" procedure applied simply consisted of a scaling factor independent of temperature, tuned so to obtain the best superposition with the ^{13}C chemical shift anisotropies NMR results, especially far from the nematic-isotropic transition. The four sets of data obtained after normalization almost coincide for both liquid crystals throughout their nematic ranges, in agreement with previous findings (Supporting Information).[5,6] The scaling factors giving the best agreement among the four sets of data

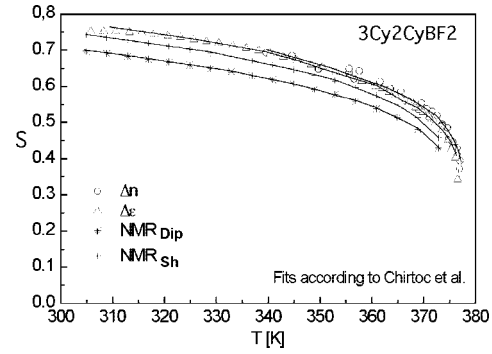

Figure 13. Order parameters S_{zz} in the nematic phase of **3Cy2CyBF2** determined from optical (Δn), dielectric ($\Delta\epsilon$), ^{13}C-^{19}F dipolar couplings (NMR_{Dip}) and ^{13}C chemical shifts (NMR_{Sh}) data. The lines refer to the fittings of the experimental data using Chirtoc et al. equation,[40] corresponding to the best fitting parameters reported in Table 1 of the Supporting Information material.

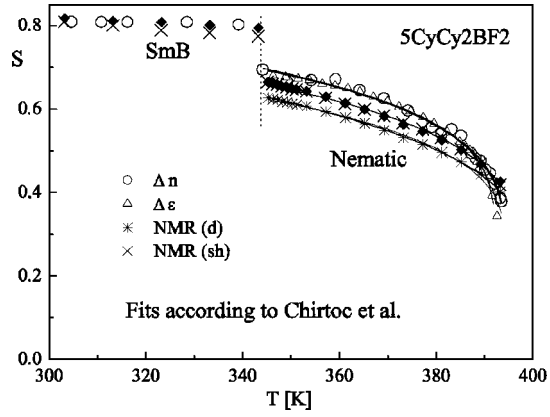

Figure 14. Order parameters S_{zz} in the nematic and smectic B phases of **5CyCy2BF2** determined from optical (Δn), dielectric ($\Delta\epsilon$), ^{13}C-^{19}F dipolar couplings (NMR_{Dip}) and ^{13}C chemical shifts (NMR_{Sh}) data. The lines refer to the fittings of the experimental data using Chirtoc et al. equation,[40] corresponding to the best fitting parameters reported in Table 1 of the Supporting Information material.

TABLE 5: Principal Values of δ Tensors (ppm) for Each ^{13}C Nucleus in the Fluorinated Aromatic Cores of 3Cy2CyBF2 and 5CyCy2BF2[a]

	3Cy2CyBF2				5CyCy2BF2			
	δ_{xx}	δ_{yy}	δ_{zz}	θ	δ_{xx}	δ_{yy}	δ_{zz}	θ
C1	150.3	87.7	211.1	11.9	153.8	89.6	211.5	7.7
C2	150.9	88.9	215.0	65.9	152.6	90.6	216.8	63.3
C3	131.4	14.9	197.8	114.8	133.9	17.2	200.0	115.9
C4	192.5	16.0	229.1	175.1	181.8	12.2	230.0	178.9
C5	123.7	24.1	221.3	−122.7	123.8	24.1	221.4	−121.9
C6	132.3	16.6	200.9	−57.2	132.5	16.8	201.1	−61.1

[a] θ is the angle between the *z*-axis of the chemical shift principal axes frame and the para axis of the relevant aromatic frame (passing through carbons C1 and C4).

were: 0.939, 0.955, and 1.066 (**3Cy2CyBF2**); 0.941, 0.941, and 1.048 (**5CyCy2BF2**) for optical, dielectric, and ^{13}C-^{19}F dipolar couplings, respectively. If the differences in the trends obtained from dielectric, optical, and ^{13}C chemical shift anisotropies could be ascribed only to the different frames where the S_{zz} order parameters were defined, then the *z*-axes of the dielectric and optical frames should be almost coincident, and they should differ by an angle of about 11 ± 1 and $8 \pm 1°$ with respect to the NMR *z*-axis (phenyl para axis) for **3Cy2CyBF2** and **5CyCy2BF2**, respectively. These values are very similar to those previously found for **3CyHeBF** and **3CyCyBF2**.[4] The order

biaxiality ($S_{xx} - S_{yy}$) could be determined from the NMR analyses at the different temperatures for both compounds. For **3Cy2CyBF2** the biaxiality evaluated from ^{13}C-^{19}F dipolar splittings and ^{13}C chemical shift anisotropies was about 10−13% of S_{zz} in the whole nematic range. For **5CyCy2BF2**, in its nematic phase these values were 10−15% (from dipolar splittings) and 20−25% (from chemical shift anisotropies), while in its smectic B were sensibly lower, about 9 and 6%, respectively. The low biaxiality observed here, in the SmB phase of **5CyCy2BF2**, is in agreement with the results previously obtained for FAB-OC6.[41] A possible explanation for this behavior can be found in the peculiar dynamics of SmB phases, where a fast rotation of the molecule about its long axis (spinning) is typically present along with a very hindered molecular tumbling (several orders of magnitudes slower than in nematic phases), so to confer an average cylindrical shape to the mesogenic core.[41] In a previous study[4] on two similar fluorinated liquid crystals, the biaxiality was found to be about 5% throughout their nematic ranges. This could suggest a role in generating some order biaxiality, as sensed by the aromatic fragment, played by the increased flexibility generated by the CH_2CH_2 bridging group (linking one cyclohexylic unit with either the other cyclohexyl or the phenyl group), the presence of which represents the main structural difference among the compounds studied here and those of the previous study. Moreover, the highest biaxiality detected by NMR for **5CyCy2BF2** seems to agree with its sensibly different molecular shape, revealed by its peculiar dielectric properties, and ascribed to the location of the CH_2CH_2 bridging group.[42] In the smectic B phase of **5CyCy2BF2**, a constant trend for the orientational order is observed as a function of temperature. This trend is commonly found for B phases (smectic B and crystal B),[41,43,44] and it is probably due to the fact that orientational order no longer acts as a heat sink. In our case, the the S_{zz} order parameter reaches an asymptotic value of about 0.8, in agreement with the values typically found for SmB phases,[41] and contrary to what previously observed for more ordered crystal B phases, characterized by S_{zz} values of nearly 1.0.[44]

5. Conclusions

In this paper a detailed analysis of the orientational order parameters was performed for two fluorinated liquid crystals exhibiting nematic and, in one case, smectic B phases, by means of optical, dielectric and ^{13}C NMR techniques. In the case of NMR the orientational order parameters were independently obtained from (i) ^{13}C-^{19}F dipolar splittings, taking into account the contributions arising from the anisotropic scalar interaction and possible deformations of the geometry due to harmonic vibrations, and from (ii) ^{13}C chemical shift anisotropies, by exploiting ^{13}C chemical shielding tensors calculated at GIAO-DFT level of theory. The results obtained for S_{zz} from the different methods were in very good agreement, especially for what concerns their trends versus temperature, which could be well reproduced by the Chirtoc et al. equation. A normalization procedure applied to the different sets of order parameters allowed an estimate of the angle between the reference frames used for the different techniques, or the systematic error due to different experimental errors and/or approximations in the data analysis, to be estimated. The results obtained revealed to be in excellent agreement with those previously obtained for other two fluorinated nematogens. The main difference observed in the orientational order behavior among the four fluorinated liquid crystals investigated so far concerns biaxiality, which seems to increase in the presence of a CH_2CH_2 bridging group, linking the two cyclohexylic units or cyclohexyl and phenyl rings.

Acknowledgment. This work was partially supported by the executive programme of scientific and technological co-operation between the Italian Republic and the Republic of Poland 2007−2009 (Project No. 8) and by italian PRIN 2005 035119. The authors are grateful to Professor Benedetta Mennucci for her support and helpful discussions concerning the DFT calculations.

Supporting Information Available: Trends of $\delta^{iso}(T)$, recorded by ^{13}C-NMR CP-MAS technique, for each chemically distinguished carbon of the aromatic unit of **3Cy2CyBF2** and of **5CyCy2BF2**; order parameters determined from optical, dielectric, and NMR data, fitted by using Haller equation; order parameters normalized by suitable scaling factors; best-fitting parameters for the Haller and Chirtoc equations used to reproduce the order parameters vs temperature trends. This material is available free of charge via the Internet at http://pubs.acs.org.

References and Notes

(1) Guittard, F.; Taffin de Givenchy, E.; Geribaldi, S.; Cambon, A. *J. Fluorine Chemistry* **1999**, *100*, 85.
(2) Virchow, R. *Angew. Chem., Int. Ed.* **2000**, *39*, 4216.
(3) Kirsch, P.; Huber, F.; Lenges, M.; Taugerbeck, A. *J. Fluorine Chemistry* **2001**, *112*, 69.
(4) Catalano, D.; Geppi, M.; Marini, A.; Veracini, C. A.; Urban, S.; Czub, J.; Kuczynski, W.; Dabrowsky, R. *J. Phys. Chem. C* **2007**, *111*, 5286.
(5) Urban, S.; Gestblom, B.; Kuczynski, B. W.; Pawlus, S.; Würflinger, A. *Phys. Chem. Chem. Phys.* **2003**, *5*, 924.
(6) Urban, S.; Würflinger, A.; Gestblom, B. *Phys. Chem. Chem. Phys.* **1999**, *1*, 2787.
(7) Veracini C. A. In *NMR of Liquid Crystals*; Emsley, J. W., Ed.; Reidel Publishing Company: Dordrecht, Germany, 1985, pp 99−121.
(8) Emsley, J. W. *Nuclear Magnetic Resonance of Liquid Crystals*; Emsley, J. W., Ed.; Reidel Publishing Company: Dordrecht, Germany, 1985, pp 379−412.
(9) Dong, R. Y. *Nuclear Magnetic Resonance of Liquid Crystals*; Springer Verlag Inc.: New York, 1994.
(10) Fung, B. M. *Prog. Nucl. Magn. Reson. Spectrosc.* **2002**, *41*, 171.
(11) Magnuson, M. L.; Tanner, L. F.; Fung, B. M. *Liq. Cryst.* **1994**, *16*, 857.
(12) Edgar, M.; Emsley, J. W.; Furby, M. I. C. *J. Magn. Reson.* **1997**, *128*, 105.
(13) Catalano, D.; Gandolfo, C.; Shilstone, G. N.; Veracini, C. A. *Liq. Cryst.* **1992**, *11*, 151.
(14) Ciampi, E.; Furby, M. I. C.; Brennan, L.; Emsley, J. W.; Lesage, A.; Emsley, L. *Liq. Cryst.* **1999**, *26*, 109.
(15) Magnuson, M. L.; Fung, B. M.; Shadt, M. *Liq. Cryst.* **1995**, *19*, 333.
(16) Kuczyński, W.; Żywucki, B.; Malecki, J. *Mol. Cryst. Liq. Cryst.* **2002**, *381*, 1.
(17) Fung, B. M.; Khitrin, A. K.; Ermolaev, K. *J. Magn. Reson.* **2000**, *142*, 97.
(18) Metz, G.; Wu, X.; Smith, S. O. *J. Magn. Reson.* **1994**, *A110*, 334.
(19) Frisch, M. J.; Trucks, G. W.; Schlegel, H. B.; Scuseria, G. E.; Robb, M. A.; Cheeseman, J. R.; Montgomery, J. A. Jr.; Vreven, T.; Kudin, K. N.; Burant, J. C.; Millam, J. M.; Iyengar, S. S.; Tomasi, J.; Barone, V.; Mennucci, B.; Cossi, M.; Scalmani, G.; Rega, N.; Petersson, G. A.; Nakatsuji, H.; Hada, M.; Ehara, M.; Toyota, K.; Fukuda, R.; Hasegawa, J.; Ishida, M.; Nakajima, T.; Honda, Y.; Kitao, O.; Nakai, H.; Klene, M.; Li, X.; Knox, J. E.; Hratchian, H. P.; Cross, J. B.; Adamo, C.; Jaramillo, J.; Gomperts, R.; Stratmann, R. E.; Yazyev, O.; Austin, A. J.; Cammi, R.; Pomelli, C.; Ochterski, J. W.; Ayala, P. Y.; Morokuma, K.; Voth, G. A.; Salvador, P.; Dannenberg, J. J.; Zakrzewski, V. G.; Dapprich, S.; Daniels, A. D.; Strain, M. C.; Farkas, O.; Malick, D. K.; Rabuck, A. D.; Raghavachari, K.; Foresman, J. B.; Ortiz, J. V.; Cui, Q.; Baboul, A. G.; Clifford, S.; Cioslowski, J.; Stefanov, B. B.; Liu, G.; Liashenko, A.; Piskorz, P.; Komaromi, I.; Martin, R. L.; Fox, D. J.; Keith, T.; Al-Laham, M. A.; Peng, C. Y.; Nanayakkara, A.; Challacombe, M.; Gill, P. M. W.; Johnson, B.; Chen, W.; Wong, M. W.; Gonzalez, C.; Pople, J. A.; *Gaussian 03*, rev. B.05; Gaussian, Inc.: Pittsburgh, PA, 2003.
(20) *CS Mopac Pro TM*; CambridgeSoft Corporation: Cambridge, Massachusetts, 1996−1999.
(21) (a) Becke, A. D. *Phys. Rev. A: At., Mol., Opt. Phys.* **1988**, *38*, 3098. (b) Lee, C.; Yang, W.; Parr, R. G. *Phys. Rev. B: Condens. Matter* **1988**, *37*, 785. (c) Stephens, P. J.; Devlin, F. J.; Chabalowski, C. H.; Frisch, M. *J. Phys. Chem.* **1994**, *98*, 11623.

(22) (a) Perdew, J. P. In *Electronic Structure of Solids*; Ziesche, P.; Eschig, H., Eds.; Akademie Verlag: Berlin, 1991; p 11. (b) Adamo, C.; Barone, V. *J. Chem. Phys.* **1998**, *108*, 664. (c) Lynch, B. J.; Zhao, Y.; Truhlar, D. G. *J. Phys. Chem. A* **2003**, *107*, 1384.

(23) Ditchfield, R. *Mol. Phys.* **1974**, *27*, 789.

(24) (a) Minkin, W. I.; Osipov, O. A.; Zhdanov, Y. A. *Dipole Moments in Organic Chemistry*, Plenum Press: New York, 1970. (b) Exner, O. *Dipole Moments in Organic Chemistry*, Georg Thieme Publishers: Stuttgart, Germany, 1975.

(25) Gestblom, B. In *Relaxation Phenomena*; Haase W., Wrobel S.,Eds.; Springer: Berlin, 2003; pp 35−51.

(26) Czub, J.; Urban, S.; Dabrowski, R.; Gestblom, B. *Acta Phys. Pol.* **2005**, *107A*, 947.

(27) Maier, W.; Meier, G. *Z. Naturforsch.* **1961**, *16a*, 262–470.

(28) Kresse, H. *Adv. Liq. Cryst.* **1983**, *6*, 109.

(29) Urban, S.; Gestblom, B. Pawlus, S. *Z. Naturforsch.* **2003**, *58a*, 357.

(30) Czub, J.; Urban, S.; Würflinger, A. *Liq. Cryst.* **2006**, *33*, 85.

(31) Dunmur, D. A. *Liq. Cryst.* **2005**, *32*, 1379.

(32) Jadzyn, J.; Czerkas, S.; Czechowski, G.; Burczyk, A.; Dabrowski, R. *Liq. Cryst.* **1999**, *26*, 437.

(33) Klasen, M.; Bremer, M.; Götz, A.; Manabe, A.; Naemura, S.; Tarumi, K. *Jpn. J. Appl. Phys.* **1998**, *37*, L945.

(34) Haller, I. V. *Prog. Solid State Chem.* **1975**, *10*, 103.

(35) Wray, V.; Ernst, L.; Lustig, E. *J. Magn. Reson.* **1977**, *27*, 1.

(36) Vaara, J.; Jokisaari, J.; Wasylishen, R. E.; Bryce, D. L. *Prog. Nucl. Magn. Reson. Spectrosc.* **2002**, *41*, 233.

(37) Vaara, J.; Kaski, J.; Jokisaari, J. *J. Phys. Chem. A* **1999**, *103*, 5675.

(38) Lucas, N. J. D. *Mol. Phys.* **1971**, *22*, 233.

(39) Dong, R. Y.; Geppi, M.; Marini, A.; Hamplova, V.; Kaspar, M.; Veracini, C. A.; Zhang, Y. *J. Phys. Chem. B* **2007**, *111*, 9787.

(40) Chirtoc, I.; Chirtoc, M.; Glorieux, C.; Thoen, J. *Liq. Cryst.* **2004**, *31*, 229.

(41) Calucci, L.; Geppi, M.; Veracini, C. A.; Forte, C.; Gandolfo, C. *Mol. Cryst. Liq. Cryst.* **1997**, *303*, 415.

(42) Czub, J.; Urban, S.; Geppi, M.; Marini, A. *Liq. Cryst.* **2008**, *35*, 527.

(43) Catalano, D.; Gandolfo, C.; Shilstone, G. N.; Veracini, C. A. *Liq. Cryst.* **1992**, *11*, 151.

(44) Calucci, L.; Francescangeli, O.; Gandolfo, C.; Komitov, L.; Veracini, C. A. *Liq. Cryst.* **1997**, *22*, 99.

JP800378G